Science of the Total Environment 828 (2022) 154421

Contents lists available at ScienceDirect

Science of the Total Environment

journal homepage: www.elsevier.com/locate/scitotenv

Towards climate-robust water quality management: Testing the efficacy of different eutrophication control measures during a heatwave in an urban canal

Qing Zhan [a,*], Sven Teurlincx [a], Frank van Herpen [b,c], Nandini Vasantha Raman [a,d], Miquel Lürling [d], Guido Waajen [e], Lisette N. de Senerpont Domis [a,d]

[a] Department of Aquatic Ecology, Netherlands Institute of Ecology (NIOO-KNAW), P.O. Box 50, 6708 PB Wageningen, the Netherlands
[b] Royal HaskoningDHV, P.O. Box 1132, 3800 BC Amersfoort, the Netherlands
[c] Water Authority Aa en Maas, P.O. Box 5049, 5201 GA 's-Hertogenbosch, the Netherlands
[d] Department of Aquatic Ecology and Water Quality Management, Wageningen University & Research, P.O. Box 47, 6708 PB Wageningen, the Netherlands
[e] Water Authority Brabantse Delta, P.O. Box 5520, 4801 DZ Breda, the Netherlands

HIGHLIGHTS

- Climate change may hamper our current restoration efforts.
- We tested four measures focusing on controlling internal loading in an urban canal.
- We evaluated the effect of an extreme heatwave on the efficacy of the measures.
- The four measures were unable to mitigate the negative heatwave impacts.
- Heatwaves lock P in a biological loop, hampering the efficacy of solid P sorbents.

GRAPHICAL ABSTRACT

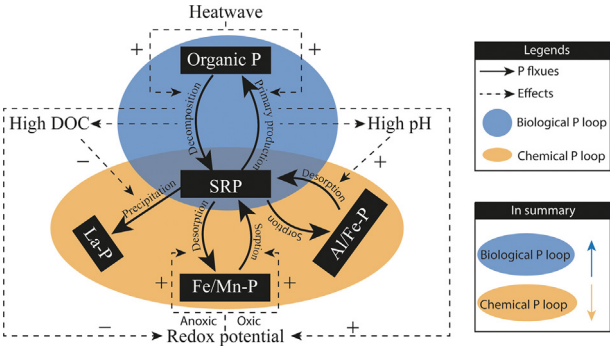

ARTICLE INFO

Article history:
Received 30 November 2021
Received in revised form 25 February 2022
Accepted 5 March 2022
Available online 9 March 2022

Editor: Fernando A.L. Pacheco

Keywords:
Lake restoration
Extreme climatic events
Iron lime sludge
Dredging
Phoslock®
Algal blooms

ABSTRACT

Harmful algal blooms are symptomatic of eutrophication and lead to deterioration of water quality and ecosystem services. Extreme climatic events could enhance eutrophication resulting in more severe nuisance algal blooms, while they also may hamper current restoration efforts aimed to reduce nutrient loads. Evaluation of restoration measures on their efficacy under climate change is essential for effective water management. We conducted a two-month mesocosm experiment in a hypertrophic urban canal focussing on the reduction of sediment phosphorus (P)-release. We tested the efficacy of four interventions, measuring phytoplankton biomass, nutrients in water and sediment. The measures included sediment dredging, water column aeration and application of P-sorbents (lanthanum-modified bentonite - Phoslock® and iron-lime sludge, a by-product from drinking water production). An extreme heatwave (with the highest daily maximum air temperature up to 40.7 °C) was recorded in the middle of our experiment. This extreme heatwave was used for the evaluation of heatwave-induced impacts. Dredging and lanthanum modified bentonite exhibited the largest efficacy in reducing phytoplankton and cyanobacteria biomass and improving water clarity, followed by iron-lime sludge, whereas aeration did not show an effect. The heatwave negatively impacted all four measures, with increased nutrient releases and consequently increased phytoplankton biomass and decreased water clarity compared to the pre-heatwave phase. We propose a conceptual model suggesting that the heatwave locks

Abbreviations: Phoslock®-Lanthanum Modified Bentonite, LMB; Soluble Reactive Phosphorus, SRP; Chlorophyll a, Chl-a; Greenhouse Gas, GHG; Dissolved Organic Carbon, DOC; Linear Mixed Effect model, LME; Principle Response Curve, PRC.

* Corresponding author.
E-mail address: Q.Zhan@nioo.knaw.nl (Q. Zhan).

http://dx.doi.org/10.1016/j.scitotenv.2022.154421

nutrients within the biological P loop, which is the exchange between labile P and organic P, while the P fraction in the chemical P loop will be decreased. As a consequence, the efficacy of chemical agents targeting P-reduction by chemical binding will be hampered by heatwaves. Our study indicates that current restoration measures might be challenged in a future with more frequent and intense heatwaves.

1. Introduction

Eutrophication, defined by over-enrichment of nutrients resulting in increased primary production, is identified as one of the key drivers of water quality deterioration in inland waters across the globe (Carpenter et al., 1999). Eutrophication of a water body can hamper provisioning of ecosystem services by a series of symptoms, e.g. accumulation of phytoplankton biomass in the water column, malodour, and oxygen depletion resulting in fish kill (Smith and Schindler, 2009). Furthermore, some cyanobacterial species can produce toxins, which pose a direct health risk to animals and humans (Chorus et al., 2000). From previous experimental and modelling studies it has been well-established that through reduction of nutrient loading degraded systems can be restored to a clear water state (Janse, 2005; Waajen, 2017).

Nutrient loading (nitrogen and phosphorus) can originate from external sources in the watershed as well as from internal lake sediments. Lakes sediments are often enriched with nutrients after years of accumulation and under certain conditions these sediment nutrients will be released into the water column (Søndergaard et al., 2013). While external loading can be controlled through e.g., watershed management and water treatment, in-lake measures that target sediment nutrient release are becoming inevitable as many studies have demonstrated that a sole reduction of external loading without control of internal loading is not efficient (Lürling and Mucci, 2020; Spears et al., 2016).

While external load control will mostly reduce both nitrogen (N) and phosphorus (P), in-lake nutrient reduction often focuses on P, as P can be made limiting more easily than N (Schindler et al., 2008). It has increasingly been accepted that drastic reduction of P release from sediments is critical for long-lasting eutrophication control (Carpenter, 2008). Bioavailabilities of phosphorus differ among various sediment P forms (Cavalcante et al., 2018). In general, the mobile P pool is comprised of forms that are easily available, such as P dissolved in pore water (measured as Soluble Reactive Phosphorus, i.e. SRP), P loosely adsorbed to FeOOH and $CaCO_3$ surfaces, P that can become available rapidly under anoxic conditions (i.e. redox-sensitive P bound to oxidized Iron and Manganese), and P that will gradually become available due to mineralization of organic matter (Hupfer et al., 2009). P adsorbed to Aluminium (Al) and Iron (Fe) oxy/hydroxides and P in Al and Fe (hydroxy)phosphates will only become available when phosphate is exchanged with hydroxyl ions at high pH (Boström, 1984). Acid-soluble and refractory organic P, P in calcium-phosphate minerals, and non-extractable mineral P are viewed as non-available (Hupfer et al., 2009).

In this study, we investigated four promising measures for their potential in mitigating internal eutrophication, including lanthanum-modified bentonite (LMB) and removal of the nutrient-rich top soil (dredging), as well as aeration and iron-lime sludge amendment. The four restoration measures have variable mode of actions to control eutrophication. Lanthanum-modified bentonite (LMB, also called Phoslock®), a well-established eutrophication control technique that has been applied to over 200 water bodies across a wide geographic distribution (Copetti et al., 2016), is developed to immobilize P by forming a La-P complex. This complex has proven to be poorly soluble under anoxic conditions and under a wide range of pH (6–10 tested in Kang et al., 2021; Mucci et al., 2018). This compound has been compared with other P adsorbents with respect to their P adsorption capacity and often performs better (Lin et al., 2015; Mucci et al., 2018). Some studies have evaluated it against dredging, a commonly used measure that removes the organic- and nutrient-rich top sediment layer. The results are not conclusive, as one study observed that LMB was less effective in removing P compared to dredging (Lürling and Faassen, 2012), whereas another study found that LMB was more effective than dredging (Yin et al., 2021). However, dredging in general is more expensive than the application of LMB (Lürling and Faassen, 2012). Aeration, as a measure of artificial oxygenation of the water column, aims at enhancing the natural capacity of the system in binding phosphorus through reduction in the concentrations of reduced forms of iron and manganese (Cowell et al., 1987; Yuan et al., 2020). Iron-lime sludge, a by-product from drinking water production, has P-adsorption capacity through the presence of iron (Fe) and calcium (Ca) (Babin et al., 1994; Golterman, 1997; Smolders et al., 2008). P bound to oxidized iron is redox-sensitive and can be remobilized under anoxic condition (Gächter and Müller, 2003), and P bound to reduced iron is suffering from sulphide which binds more strongly to reduced iron than to P (Geurts et al., 2010). The Ca in the iron sludge may bind P under elevated pH. These Ca-P minerals are stable under most natural conditions, but P bound by Ca can be released under acidic conditions (Huang et al., 2005). As a waste product from water treatment this sludge is economically favourable compared to dredging and lanthanum modified bentonite (LMB).

To compare the efficacy of these four measures in a near-realistic environment, we conducted a two-month mesocosm experiment in a hypertrophic urban canal. Such mesocosm experimental settings have proven to be a valuable approach for testing the efficacy of various ecological restoration measures in urban waterways in previous studies (Waajen et al., 2017). Mesocosm studies represent a near-realistic level of environmental complexity while allowing for a replicated design with well-defined treatments. Shallow water bodies are the most abundant freshwater ecosystems (Verpoorter et al., 2014) and provide important ecological and societal services including recreation, water and nutrients retention, microclimate regulation and biodiversity reservoir (Biggs et al., 2017; Bolund and Hunhammar, 1999). Urban canals and ponds are examples of such shallow freshwater ecosystems that, due to their close proximity to humans, are both valuable for ecosystem service provisioning as well as exposed to high levels of anthropogenic stressors (Noble and Hassall, 2015; Teurlincx et al., 2019). They are often nutrient-rich and regularly suffering from blooms of nuisance algae (Waajen et al., 2014).

The main objectives of this study are: (i) comparing the efficacy of four intervention measures in reducing nutrient releases and controlling eutrophication; (ii) evaluating the heatwave impacts on the efficacy of these four intervention measures; (iii) proposing a conceptual model that provides routes through which measures to mitigate sediment phosphorus release might be affected by heatwaves. We propose the following hypotheses regarding the efficacy of the four measures: Hypothesis 1) Dredging and lanthanum modified bentonite (LMB), via reducing mobile P effluxes from the sediments, will be the most effective measures in reducing phytoplankton biomass; Hypothesis 2) Iron-lime sludge will be less effective in reducing sediment P release because it is both redox-sensitive and pH-sensitive; Hypothesis 3) Aeration -although widely used- is not effective for P-reduction as in such a shallow system air pumping can lead to enhanced sediment resuspension promoting nutrient release (Visser et al., 2016).

In future climate conditions the efficacy of the current restoration measures might be hampered by extreme climate events posing a sudden and severe disturbance to lakes (Stockwell et al., 2020; Woolway et al., 2020). For instance, lake heatwaves, defined as periods of extremely warm surface water temperature, are anticipated to increase both in frequency and intensity in future (Woolway et al., 2021). The heatwave impacts are expected to be especially relevant to shallow water systems as their temperatures are highly related to the air temperature (Mooij et al., 2008). Release of organic

P can be enhanced with increasing temperatures owing to accelerated decomposition rates, whereas the redox sensitive P will be rapidly freed under anoxia. Such conditions, higher temperatures, and stronger bottom water anoxia (Jankowski et al., 2006) are consequences of climate change. In addition, warming is also seen as an important factor that promotes algal blooms (Paerl and Huisman, 2008) and therewith could lead to elevated pH in surface waters. The climate impact-related factors temperature, redox, and pH influence phosphate diagenesis and thus how much P can become available (Holtan et al., 1988). Less evidence, however, is collected from field studies on the impact of heatwaves on the effectiveness of restoration measures. In the middle of our 2 months mesocosm experiment we recorded an extreme heatwave, which provided the opportunity for evaluation of heatwave impacts on the efficacy of the four restoration measures.

We hypothesize that this heatwave, through its impacts on the oxygen content of the water body (Jeppesen et al., 2021), could hamper the efficacy of iron-lime sludge (Hypothesis 4). As a previous short-term laboratory experiment demonstrated that the efficacy of Lanthanum modified bentonite can be hampered upon exposure to a heatwave (Zhan et al., 2021), we hypothesize that the induced P-release will compromise the efficacy of Lanthanum modified bentonite (Hypothesis 5). Since dredging is designed to remove the nutrient-rich top layer of the sediments, we expect no effect of the heatwave on the efficacy of the dredging treatments (Hypothesis 6).

2. Methods and materials

2.1. Experimental set-up

A mesocosm experiment was carried out in a shallow urban canal (max depth ca 3 m) situated in the South of the Netherlands in the municipality of Geertruidenberg (coordinates in DMS: 51°42′12.0″N 4°51′40.8″E). The canal has a stable water level owing to regulation of inlet waters (full capacity = 0.06 m^3/s) by local water managers. Drought is therefore not considered a problem for this system throughout the year. The sediments at this study site were sampled and analysed in September of 2018 (1 year prior to the experiment) for determination of the chemical adsorbent dosages applied in the mesocosm experiment. The P fractions in the top 20 cm sediments (communicating depth) were determined by a sequential P-fractionation analysis (Hupfer et al., 2009; Psenner et al., 1984), where the following fractions were determined: the P dissolved in the pore water (SRP), the redox-sensitive bound P (bound to Iron or Manganese), the organic P, the acidity-sensitive P (bound to Aluminium or Calcium) and the refractory P.

The mesocosm experiment was carried out from 25-06-2019 to 19-09-2019. In total, 20 mesocosms (clear Perspex cylinders with height: 2.25 m; diameter: 1.05 m) were exposed to four measures and one control treatment, yielding 5 treatments × 4 replicates. To allow for air-water interactions and sediment-water interactions, the mesocosms were open at the top and bottom, see Fig. 1a. The treatments were assigned randomly to the mesocosms to account for the heterogeneity of sediment and water conditions. The mesocosms were inserted ca. 30 cm deep in the sediment, with an overlaying water layer of ca. 1.6 m. The four measures tested include: iron-lime sludge (drinking water production by-products), lanthanum modified bentonite (LMB), aeration and dredging. The doses and/or application of these four measures are introduced in Section 2.2 below.

At the mid of our experiment (22th of July–27th of July), an extreme heatwave event –maximum air temperature 25.0 °C or higher– was recorded by Royal Netherlands Meteorological Institute (KNMI, https://www.knmi.nl/nederland-nu/klimatologie/lijsten/hittegolven). This heatwave had 4 tropical days (maximum temperature 30.0 °C or higher) with a maximum of 40.7 °C (from the nearby weather station Gilze-Rijen, https://www.knmi.nl/nederland-nu/klimatologie/daggegevens), which was the highest recorded heatwave temperature since 1901 (the average Dutch summer temperature ≈ 21.0 °C). During each sampling event we monitored the water temperature, recording a time series of water temperature dynamics at a time interval of 2–3 weeks. In addition to the measurements, we ran FLake (http://www.flake.igb-berlin.de/), an open-resource model, specifically designed to evaluate climate scenario's influences on inland waters and numerically predict water temperature and mixing regime (Shatwell et al., 2019). This process-based model has a high level of parametrization, is well validated for inland waters and thus allowed us to simulate water temperature dynamics at a daily base. Details on how we configured the FLake model for the Geertruidenberg canal system can be found in the supplemental information Section 1. All the model parameters are summarized in table SI-1. Based on the measured and simulated temperature dynamics (Fig. 1b), we incorporated the sampling event prior (12th of July) and post heatwave (7th of August) in our analysis of the impacts of an extreme heatwave. In such a way we included both the rising and falling limb of the extreme heatwave. We refer to this period as the 'heatwave phase' from hereon. Note that this heatwave phase differs from the definition of heatwave period by KNMI, which is defined as a succession of at least 5 summer days (maximum air temperature 25.0 °C or higher) in De Bilt (the headquarters of KNMI), of which at least three are tropical (maximum air temperature 30.0 °C or higher).

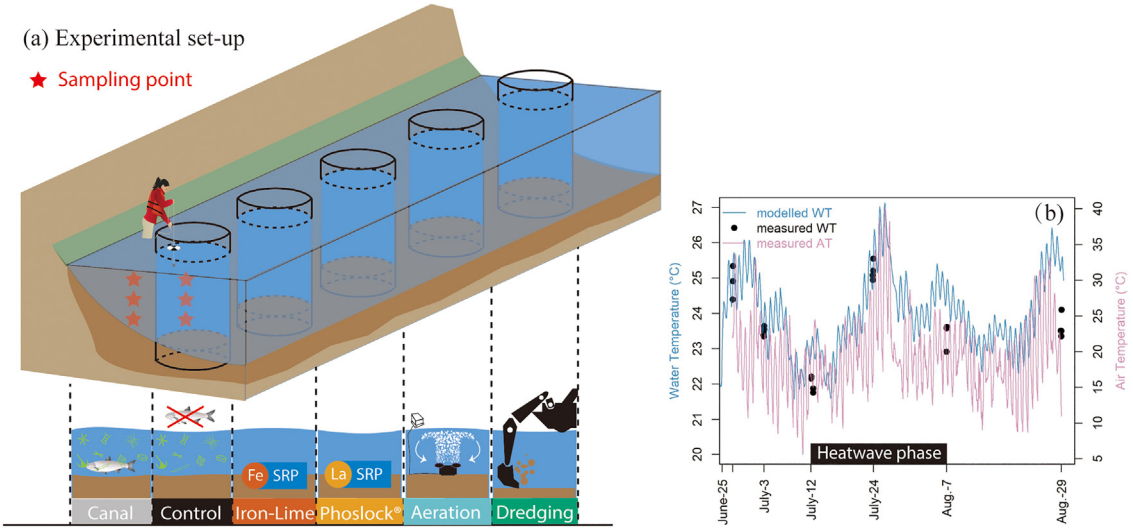

Fig. 1. (a) Experimental set-up; (b) Dynamics of monitored air temperature (AT; in purple line) and modelled water temperature (WT; in blue line) and measured water temperature (WT; in black points). As we observed no difference in the water temperature in the mesocosms and the surrounding canal water, we proceeded with displaying the mean of the measured temperatures.

2.2. Restoration treatments

The sediment was characterized as fluffy with a density of 1.21 ± 0.04 kg/L. The sediment P fractionation analysis showed that the sediment is nutrient-rich. This analysis showed that the P pool available for growth of primary producers (the sum of pore-water P, redox-sensitive P, and organic P) was 234.15 ± 9.88 μg P/g. When taking the acidity-sensitive P that becomes bio-available at very high or low pH, the mobile P averages to 291.32 ± 10.43 μg P/g. The amount of P in pore water was marginal. The redox sensitive P and organic P were the most abundant P species in our sediments.

2.2.1. Lanthanum modified bentonite (also called Phoslock®)

The dosage of lanthanum modified bentonite (LMB) was based on the amount of potentially releasable P (=291.32 ± 10.43 μg P/g, including pore-water P, redox-sensitive P, organic P, and pH-sensitive P) in the top 5 cm layer of the sediment (as in Lürling et al., 2017; Yin et al., 2021), and weight ratio of LMB:P of 230:1 (as based on Lürling et al., 2014). The water column total P (=SRP + particulate P) was assumed to be negligible compared to the sediment P pools and thus not included into the determination of LMB dose. As such, we added 1.35 kg of LMB as a slurry to the bottom of each of the four mesocosms using a 1.5 m tube in a rotating motion in two doses on 25-06-2019 (by 89% = 1.2 kg LMB) and 26-06-2019 (by the remaining 11% = 0.15 kg LMB), forming a layer of approximately 1 cm thick of LMB on the top of sediments.

2.2.2. Iron-lime sludge

On 25-06-2019, 13.4 kg of iron-lime sludge, collected from drinking water treatment plant Veghel, was applied as a slurry via a 1.5 m tube onto the sediments of each of the four mesocosms, resulting in a layer of approximately 1 cm thick of sludge. Measured concentrations of various elements in the iron-lime sludge can be found in supplemental Table SI-2. Our dose resulted in an approximate addition of 495.4 g of Calcium, 215.0 g of Iron, 21.8 g of P, and 1.1 g of Sulphur to the treated mesocosms. The P present in the iron-lime sludge has proven to not hamper eutrophication control in previous experiments (Remke et al., 2018), owing to its favourable Fe/P and Ca/P ratios. Note that phosphorus adsorption capacity of this material is not only dependent on sludge composition (i.e. Ca/Fe, Fe/S) but also on other environmental conditions including redox conditions and pH levels, resulting in a contextual dose-response relationship. As a compromise, we followed the dosage that has proven to be successful in locking P in previous experiments implemented in two eutrophic Dutch ponds (Remke et al., 2018).

2.2.3. Dredging

On 25-06-2019, for dredging treatments ca. 30 cm of the silt layer of the sediments were mechanically removed with an excavator on a pontoon, before four mesocosms were pushed into the dredged sediments. This method was applied in another mesocosm experiment testing the effect of dredging and Lanthanum modified bentonite in controlling phytoplankton nuisance in a hypertrophic pond (Lürling et al., 2017). Removal of top sediments resulted in the top edge of the four dredged mesocosms being slightly lower relative to the non-dredged mesocosms (<30 cm). At all times during the experiment, there was sufficient headspace in the dredged mesocosms to prevent exchange with the surrounding canal water.

2.2.4. Aeration

Aeration tiles (AIRDisc 250®) with a fixed airflow of 250 L h^{-1} were placed on the sediment and turned on at 26-06-2019, enriching the water column with pressurized air. The aeration rate was set to allow for sufficient oxygenation while not creating air bubbles which can negatively impact zooplankton (Cowell et al., 1987).

2.3. Water & sediment sampling

We sampled each mesocosm and the canal water 6–7 times at a time interval of 2–3 weeks over the experimental period for a suite of water quality parameters, including analyses of phytoplankton (green algae, diatoms and cyanobacteria), macronutrients (phosphorus and nitrogen), water transparency (Secchi depth) and metals (manganese-Mn, aluminium-Al, lanthanum-La, iron-Fe). All sampling events were conducted at midday between 12 pm and 14 pm, such that our oxygen results did not reflect differences in primary productivity taking place over the course of the day, which can be substantial in a hypertrophic system such as ours. A sample of the top 50 cm of the water layer was taken for measurements of chlorophyll-a fluorescence using a Phyto-PAM fluorometer (Walz, Effeltrich, Germany), as a proxy of the phytoplankton biomass (Lürling et al., 2018), with the chlorophyll-a fluorescence of cyanobacteria, green algae and diatoms differentiated by blue, green and brown signals in emission lights, respectively (Cabrerizo et al., 2020). After water samples were filtered over prewashed GF/F filters (Whatman, Maidstone, U.K.), dissolved phosphorus (SRP), nitrite (NO_2-N), nitrate (NO_3-N) and ammonium (NH_4-N) were determined in the filtrate using a QuAAtro39 Auto-Analyzer (SEAL Analytical Ltd., Southampton, U.K.). The filters containing the residue were further used for determination of particulate phosphorus (PP) using a digestion step. In short, we incinerated the filters at 550 °C for 20 min, after which the filters were autoclaved with a 2% potassium persulfate solution at 121 °C for 30 min. The resulting solutions were analysed for PP concentrations using a QuAAtro39 Auto-Analyzer (SEAL Analytical Ltd., Southampton, U.K.). The SRP and PP added up to be the total phosphorus (TP). The transparency of the water column was determined on site with a Secchi disc. We used inductively coupled plasma - optical emission spectrometry (ICP-OES, Thermo ICAP 6500-duo ICP) for measurement of total filterable metals, including Ca, Al, La, Fe. In addition, we measured depth profiles of dissolved oxygen (DO), pH using a Hydrolab multisensor probe (Hydrolab DS 5, Ott Hydromet, Colorado, United States). To control for the impact of mesocosms on the water quality, all of the above measurements were also carried out in the canal outside of the mesocosms (ca. 1 m distance).

In addition, an extra sampling of the pore water of the top 10–15 cm sediment was done using a Rhizon® soil sampler at the end of the mesocosm experiment (19-09-2019). Porewater samples were analysed using the same method and instruments described above for determination of the water concentrations of dissolved nutrients and metal elements. In addition, to gain further insight into the effect of our treatments on microbial activity and their greenhouse gas production, we followed a headspace equilibration technique (Halbedel, 2015; Magen et al., 2014) for determination of concentrations of dissolved carbon dioxide (CO_2), methane (CH_4) and nitrous oxide (N_2O) in the water column. GC-FID (Gas Chromatography-Flame Ionization Detection) was used for determining the headspace gas concentrations, and the gas concentrations in the water column were calculated based on the equilibrium relationship between water column and headspace (Zhan et al., 2021). Note that in this approach the gas fluxes through bubbling are not included.

2.4. Statistical analysis

We used a multivariate analysis method, i.e. principal response curve (PRC; Van den Brink and Braak, 1999), to visualize the overall responses (principle response) in different restoration treatments over time. In this approach, a principle variable for each restoration treatment was produced summarizing the variation in a set of response variables including Secchi depth, dissolved oxygen (DO), pH, total phosphorus (TP) and dissolved phosphorus (SRP), total chlorophyll-a (sum of chlorophyll-a of cyanobacteria, green algae, and diatoms) and cyanobacterial chlorophyll-a, which are the most relevant response variables regarding our research questions. The weights of individual response variables on the principle response curve are represented on the extra right y-axis (b_k) in the PRC diagram, indicating the contributions of individual variables to the principle response patterns. The mesocosms without restoration treatments (control)

were taken as a reference line, with its principal trajectory set to zero. As a result, the deviations of other treatments from the control mesocosms can be interpreted as an overall response to the restoration treatments (represented in the left y-axis of PRC: expressed as the coefficient of treatment response, C_{dt}) over time (x-axis). The canal water was taken as another treatment for evaluation of the potential effects of mesocosms (i.e. isolation of a water volume from the surrounding canal water). Note that the patterns of the overall responses are influenced by selection of the variables. We have selected the water quality variables that are of importance in terms of evaluation of heatwave and treatment impacts.

Further, we used linear mixed effect models to test for significant differences in the response parameters between the treatments over time (LME; Lindstrom and Bates, 1988). The linear mixed effect model allows for testing both fixed effects as well as random effects. Mesocosm identity was included in LME as a random effect to account for the heterogeneity between different mesocosm sites. To evaluate the treatment-related changes in response variables over the whole experimental period, we included the restoration treatments and the experimental time as fixed effects. In addition, to evaluate the effect of nutrient availability for the dynamics of algal biomass, dissolved phosphorus (SRP) and dissolved ammonium (NH_4-N) were included as predictor variables in the LME model for the response variables total chlorophyll-a and cyanobacteria chlorophyll-a.

To evaluate the effect of occurrence of an extreme heatwave on the efficacy of the different measures, observed water temperature was included as an additional fixed effect during the heatwave phase (12th of July–7th of August). In this analysis, time was excluded as there were only three sampling points during this period. We regard this as a solution for evaluating heatwave impacts in a field experiment where a control treatment of heatwave is not possible.

We used depth-integrated values for the variables DO and pH in the data analysis, as the depth profiles of these variables showed limited variability with depth. We confirmed this absence of stratification during the experimental period with our FLake simulation results.

We used a Shapiro–Wilk test (Ghasemi and Zahediasl, 2012) to test for normality of model residuals and if needed, different data transformation methods were applied, including logarithmic, reciprocal and square root. Breusch Pagen test (Waldman, 1983) was used to check for heteroscedasticity of the residuals and if needed, a weighted linear mixed-effect model was carried out to correct for deviations from homoscedasticity.

To evaluate treatments effects on the nutrients in the sediment pore water (sampled at the end of the experiment), we used one-way ANOVAs. Tukey's range test was utilized to compare the means of Greenhouse Gas (GHG: CO_2, CH_4, and N_2O) concentrations between the different treatments (Tukey, 1949). All statistical analyses and data visualization were performed in R language (R Core Team, 2019). We used the packages *lubridate* (Grolemond and Wickman, 2011), *nlme* (Pinheiro et al., 2019), *dplyr* (Wickham et al., 2019), and *vegan* (Oksanen et al., 2019). In addition, we used colour-blind-friendly colour palette for visualizations of our results following Wong (2011).

3. Results

3.1. Intervention treatment effects on water quality

Our PRC model (Fig. 2) revealed that among the four restoration treatments the Lanthanum modified bentonite (LMB) groups showed the strongest mitigation potential relative to the control treatments, followed by the dredging and iron-lime sludge treatments. The aeration treatment showed the least deviation from the control mesocosms, reflecting its limited potential for water quality improvement. In addition, the principal response curve of the surrounding canal water showed a distinct negative deviation from the control treatment, indicating a strong mesocosm effect on the water quality dynamics.

The response variables Secchi depth, total chlorophyll-a and cyanobacteria chlorophyll-a accounted for the largest contribution to the variation in the principle response variable, with TP, pH and DO only playing a minor role in determining the overall response patterns. Secchi depth and nutrients developed in opposite directions to the chlorophyll-a variables, pH and DO, indicating a negative correlation between these two sets of parameters.

Over the course of the experimental period, our LME model detected a significant decrease in dissolved oxygen (DO) concentrations over time, from an initial value of 11.0 ± 0.5 mg/L down to 5.7 ± 0.2 mg/L at the end of the experiment (DO log-transformed: effect of time = −0.12, $F_{1, 111} = 90.0$, $p < 0.001$, Fig. 3a). The restoration treatments did not show a significant effect on the DO dynamics.

The LME model detected a significant increase in Secchi depths over the course of the experiment (effect of time = 0.03, $F_{1, 111} = 24.8$, $p < 0.0001$, Fig. 3b). The restoration treatments also had a significant impact on Secchi depth relative to the control ($F_{5, 15} = 4.13$, $p = 0.01$), with the largest increases in transparency in the dredging treatment (by 38.5 ± 15.5%), followed by the LMB treatment (by 19.1 ± 15.1%) and the iron-lime sludge treatment (by 11.1 ± 15.0%), whereas the aeration treatment showed a decrease in Secchi depths (by 13.0 ± 15.1%). Secchi depths in mesocosms improved in comparison to the canal water (estimate of difference = −34.3, DF = 15, t-value = −1.83, $p = 0.087$). The Secchi depth in the canal

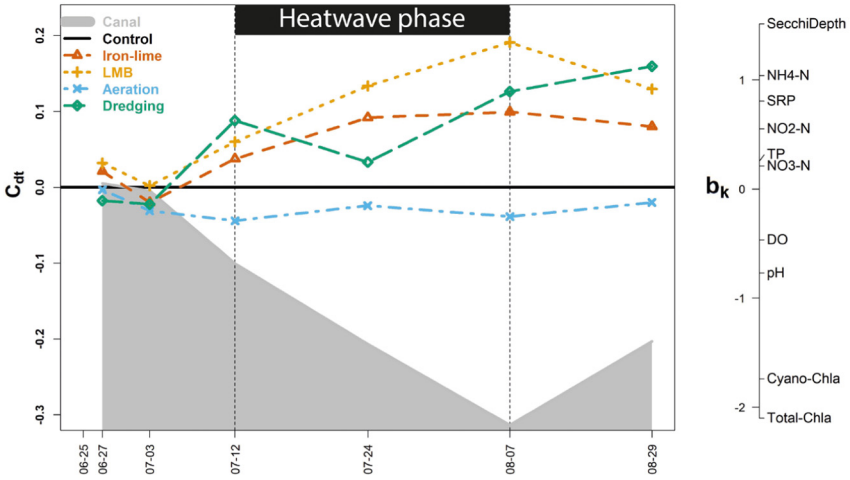

Fig. 2. Principal response curve of water quality parameters. The principal response curve model included the parameters Secchi Depth, DO, pH, total chlorophyll-a, cyanobacteria chlorophyll-a, SRP, TP, NH_4-N, NO_2-N and NO_3-N. The PRC shows the trajectory of each treatment response (coefficient of treatment response, C_{dt}) for each restoration treatment on the left y axis, with the control mesocosms trajectory set to 0. The x-axis represents time. The weights of individual water quality parameters (b_k) on the overall system response curves are displayed on the right y-axis.

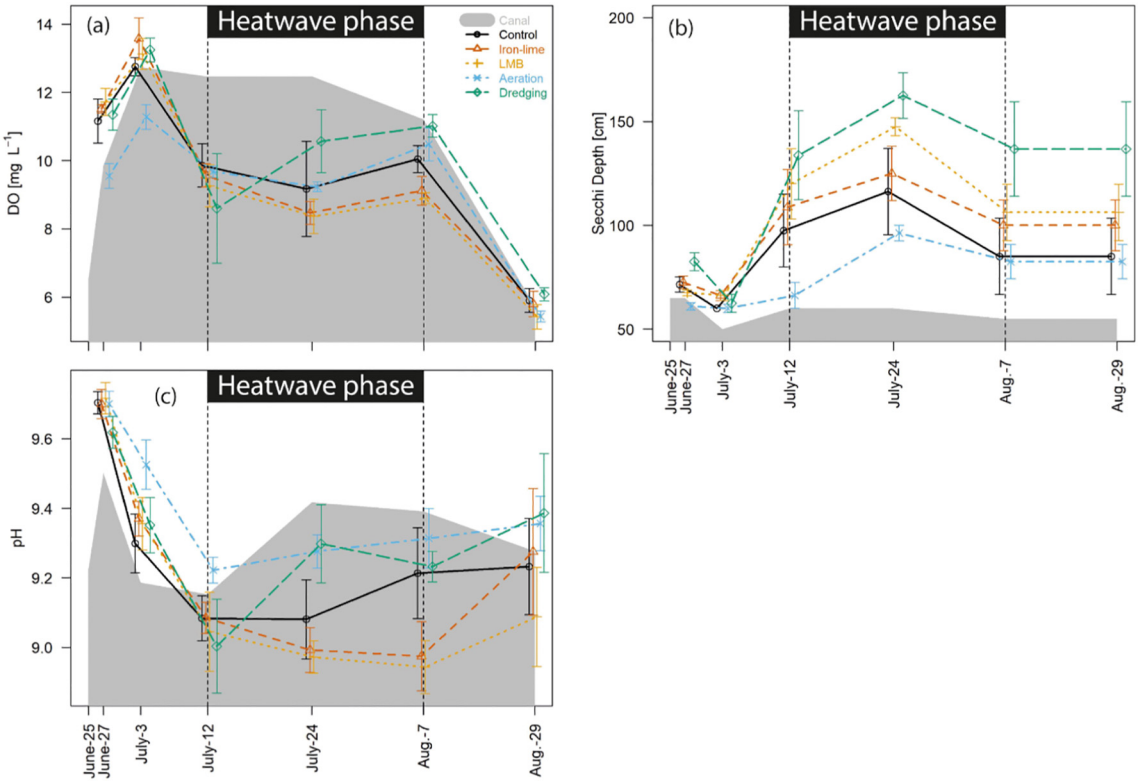

Fig. 3. Dynamics of (a) dissolved oxygen (DO), (b) Secchi depth, and (c) pH values in the water column. Error bars illustrate standard errors.

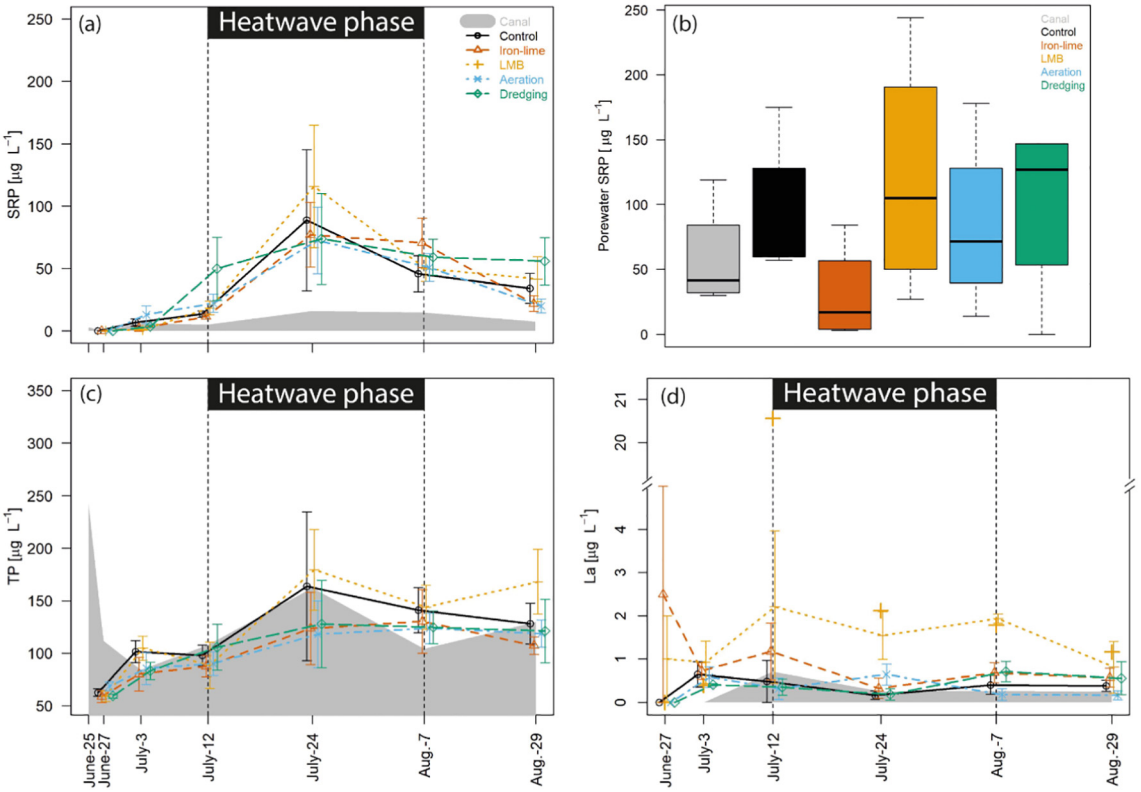

Fig. 4. Soluble reactive phosphorus (SRP) in the water column (a) and in the sediment pore water (b), total phosphorus (TP = SRP + particulate P) (c), and Lanthanum (La) concentration (d) in the water column. The La concentrations in one mesocosm ("+" points in orange colour) were represented separately, as the observed concentrations in this mesocosm strongly deviated from the rest of levels found in the other mesocosms on 12th of July. Error bars illustrate standard errors.

stayed at low levels (56.9 ± 1.2 cm) over the entire course of the experiment.

The pH levels in the water columns started at high levels (mean = 9.28 ± 0.02) and decreased significantly over time (effect of time = −0.005, $F_{1, 111} = 19.46$, $p < 0.0001$; Fig. 3c), without significant differences between the different restoration treatments.

Over the experimental period, the LME model detected a significant time effect on the dissolved phosphorus levels (SRP, estimate of time effect = 0.0007, $F_{1, 110} = 17.82$, $p < 0.0001$, Fig. 4a). The mesocosms were SRP-depleted at the start of the experiment (< 0.6 μg P/L), after which the SRP concentrations started to rise, reaching maximum concentrations of 82.2 ± 16.3 μg P/L on 24th of July. In the end of the experiment, the SRP levels decreased to 30.1 ± 5.5 μg P/L. The restoration treatments showed no significant effect on the SRP dynamics. The SRP concentrations in the canal water were lower than in the mesocosms during the experimental period (9.2 ± 2.1 μg P/L), showing no initial increase as observed in the mesocosms. At the end of the experimental period, our one-way ANOVA model detected no significant differences in the pore-water SRP concentrations between restoration treatments ($F_{5, 18} = 1.01$, $p = 0.44$; Fig. 4b). The SRP concentrations in the pore water were comparable with the maximum water column concentrations as observed on 24th of July with average concentrations of 85.7 ± 15.1 μg P/L.

The total phosphorus concentrations (TP) increased significantly over the experimental period (estimate of time effect by LME model = 0.009, $F_{1, 110} = 31.55$, $p < 0.0001$, Fig. 4c). The LME model detected no effect of the restoration treatments on TP levels, and there was no distinct difference between the TP levels in the canal water and the mesocosm water.

The LME model revealed that the lanthanum concentrations (La) in the water column of the LMB treatments were significantly higher relative to the control mesocosms (estimate of difference = 1.8 μg/L, DF = 15, t-value = 2.94, $p = 0.01$; Fig. 4d).

Over the whole experimental period, the LME model detected a significant Time × Restoration treatment effect on total chlorophyll-a concentrations ($F_{5,103} = 4.1$, $p = 0.0021$; Fig. 5a). Overall, the total chlorophyll-a concentrations started at a high level of 57.7 ± 1.9 μg/L, reaching the lowest level of 14.9 ± 5.4 μg/L at the end of July, which coincided with the peak in nutrients (Fig. 4, SRP = 82.2 ± 16.2 μg/L; Fig. S1, NH_4-N = 0.91 ± 0.07 mg/L) as observed during the heatwave phase (Fig. 1b). After the heatwave phase, the total chlorophyll-a concentrations increased with concentrations at the end of the experiment reaching levels of 44.0 ± 6.1 μg Chl-a/L. Our LME model detected a significant difference between the restoration treatments ($F_{5, 15} = 5.98$, $p = 0.0031$), with the dredging treatment resulting in a 62.5 ± 39.9% reduction in Chl-a levels relative to the control treatment. Compared with the control mesocosm, the LMB treatment reduced Chl-a levels by 48.2 ± 39.5%, while the iron-lime sludge treatment reduced Chl-a levels by 46.2 ± 41.2% by the end of the experiment. The aeration treatment showed no distinct difference with the control treatment. The control treatment had significantly lower total chlorophyll-a concentrations relative to the surrounding canal water, showing a reduction in end concentrations by 82.2 ± 41.2%. In addition, our LME model detected significant effects of nutrient availability on the total chlorophyll-a levels (estimate of SRP effect = −32.46, $F_{1,108} = 28.94$, $p < 0.0001$; estimate of NH_4-N effect = −32.04, $F_{1,108} = 27.09$, $p < 0.0001$).

For the cyanobacteria chlorophyll-a, the LME model showed an overall increase during the experimental period (estimate of time effect = 0.13, $F_{1,108} = 31.93$, $p < 0.0001$; Fig. 5b). After an initial decrease from 5.84 ± 1.88 to 0.89 ± 0.15 μg/L the concentrations increased continuously ending with a relatively high level of 10.06 ± 1.32 μg/L. The restoration treatments showed significant effects on the cyanobacteria chlorophyll-a levels ($F_{5, 15} = 5.37$, $p = 0.005$), with the largest reduction relative to the control treatment in the end concentration of cyanobacteria chlorophyll-a by the dredging treatment by 58.5 ± 33.8%, followed by the LMB treatment by 51.6 ± 32.2% and by the iron-lime sludge treatment by 40.8 ± 33.7%, whereas the aeration treatment did not reduce the cyanobacteria chlorophyll-a levels. Similar to the total chlorophyll-a measurements, the cyanobacteria chlorophyll-a concentrations in the control mesocosms had a much lower level compared to the canal water, showing a reduction of 82.8 ± 34.6%. Comparable to the results of the total chlorophyll-a LME model, the cyanobacteria chlorophyll-a LME model also detected significant effects of SRP and NH_4-N on the cyanobacteria chlorophyll-a levels (estimate of SRP effect = 9.31, $F_{1,108} = 5.28$, $p = 0.02$; estimate of NH_4-N effect = −5.08, $F_{1,108} = 6.29$, $p = 0.01$).

3.2. The heatwave effects on water quality and intervention treatment efficacy

During the heatwave phase, our LME model did not detect a significant main effect of temperature on DO concentrations. However, during the heatwave phase the restoration treatments showed a significant effect on the DO levels relative to the control treatment ($F_{5, 15} = 5.45$, $p = 0.0047$), with increased DO concentrations in the dredged treatment (by 12.3 ± 6.4%) and decreased DO concentrations in the LMB treatment (by 10.1 ± 6.4%) and iron-lime sludge treatment (by 8.5 ± 6.4%). There was no significant difference in the aeration treatment (by 2.6 ± 6.4%) relative to the control treatment. The control treatment had significantly lower DO concentrations relative to the surrounding canal water (by 19.3 ± 7.4%).

During the heatwave phase, our LME model indicated that Secchi depths increased significantly with water temperatures (main effect of temperature = 7.36, $F_{1,44} = 17.25$, $p = 0.0001$). The main effect of

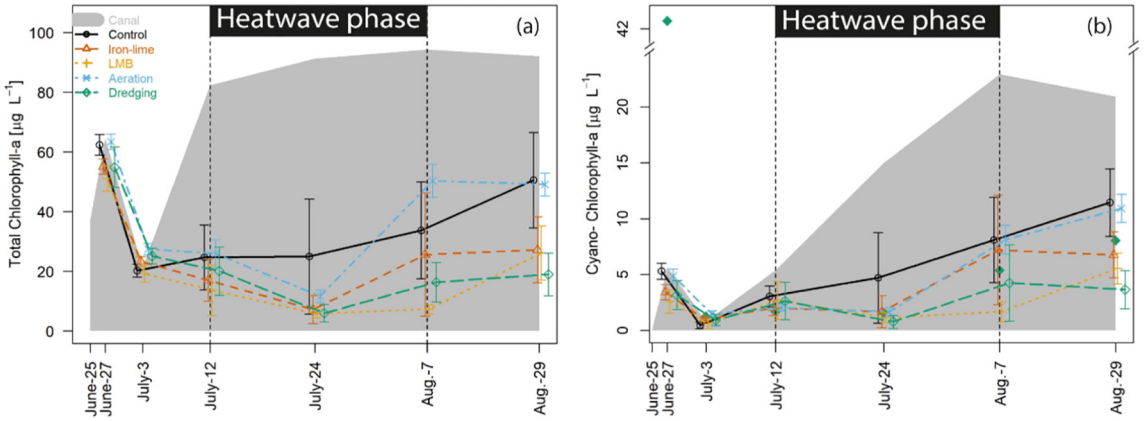

Fig. 5. Total chlorophyll-a concentration (a) and cyanobacterial chlorophyll-a concentration (b) in the water column. The cyanobacterial chlorophyll-a concentration concentrations in one mesocosm (blue-bluish green points) were represented separately, as the observed concentrations in this mesocosm strongly deviated from the rest of levels found in the other mesocosms on 27^{h} of June. Error bars illustrate standard errors.

temperature, however, was not treatment-dependent, indicating no treatments effects on the responses in water transparency to heatwave exposure.

The LME model detected a significant difference in the pH dynamics between the restoration treatments ($F_{5, 15} = 6.06$, $p < 0.003$) relative to the control treatment, with increased pH levels in the dredging treatment (by 0.77 ± 0.97%) and aeration treatment (by 1.89 ± 0.98%), and decreased pH levels in the LMB treatment (by 1.16 ± 0.97%). The iron-lime sludge treatment showed no distinct difference with the control treatment (by 0.48 ± 0.97%). The control treatment had significantly lower pH levels relative to the surrounding canal water (by 1.53 ± 1.17%). The LME model detected no main effect of temperature on the pH dynamics.

During the heatwave phase, LME model detected a positive main effect of temperature on the SRP levels (SRP log-transformed: estimate of temperature effect = 0.40, $F_{1,44} = 27.11$, $p < 0.0001$), resulting in a mean rise of 37.4 μg P/L compared to the prior-heatwave phase (days 0–16). Similar to the SRP, the TP concentrations increased with water temperatures during the heatwave phase (TP log-transformed: estimate of temperature effect = 0.089, $F_{1,44} = 4.35$, $p = 0.04$).

During the heatwave phase, LME model showed that the total chlorophyll-a levels decreased with the water temperatures (total chlorophyll-a log-transformed: estimate of temperature effect = −0.16, $F_{1,43} = 19.65$, $p = 0.0001$). Similar to the analyses of the entire experimental period (see above), the availability of NH_4-N had a significant effect on the total chlorophyll-a concentrations during the heatwave phase (total chlorophyll-a log-transformed: estimate of NH_4-N effect = −2.21, $F_{1,43} = 4.89$, $p = 0.03$). The availability of SRP, however, had no significant effect on the total chlorophyll-a levels during the heatwave phase.

During the heatwave phase, LME model detected no main effect of temperature on the development of cyanobacteria chlorophyll-a. Regarding the nutrient effects on the cyanobacteria chlorophyll-a, the effect of NH_4-N availability remained (cyanobacteria chlorophyll-a square root-transformed: estimate of NH_4-N effect = −1.34, $F_{1,43} = 8.33$, $p = 0.006$) but the SRP effect disappeared.

3.3. Treatment effects on dissolved greenhouse gas concentrations

The LMB treatment had the highest dissolved GHG concentrations at the end of the experiment, while the aeration treatment had the lowest dissolved GHG concentrations (based on Tukey test, see also Fig. 6). For instance, the LMB mesocosms had significantly increased dissolved CO_2 values in comparison to the control mesocosms (estimate of difference = 64.0 μmol/L, $p = 0.08$) and to the aerated mesocosms (estimate of difference = 90.2 μmol/L, $p = 0.01$).

With respect to the concentrations of the dissolved CH_4 at the end of the experimental period, the aerated mesocosms showed decreased values in comparison to the control mesocosms (estimate of difference = 4.3 nmol/L, $p = 0.07$) and to the iron-lime sludge mesocosms (estimate of difference = 4.5 nmol/L, $p = 0.06$); The LMB mesocosms had higher dissolved CH_4 values than the aerated mesocosms (estimate of difference = 7.9 nmol/L, $p < 0.005$) and dredged mesocosms (estimate of difference = 4.4 nmol/L, $p = 0.07$).

With respect to the concentrations of dissolved N_2O, the aerated mesocosms had significantly lower values than the control mesocosms (estimate of difference = 19.7 nmol/L, $p = 0.02$), iron-lime sludge mesocosms (estimate of difference = 18.0 nmol/L, $p = 0.05$), and LMB mesocosms (estimate of difference = 34.3 nmol/L, $p < 0.005$). In addition, the LMB mesocosms had higher dissolved N_2O concentrations than the mesocosms that were exposed to the iron-lime sludge mesocosms (estimate of difference = 16.3 nmol/L, $p = 0.08$) and the dredging mesocosms (estimate of difference = 21.8 nmol/L, $p = 0.01$).

4. Discussion

In this study, we compared four restoration measures with respect to their efficacy of reducing phytoplankton and improving water quality in an urban canal using a mesocosm approach. This type of experiments comparing different intervention measures at a near-realistic level of

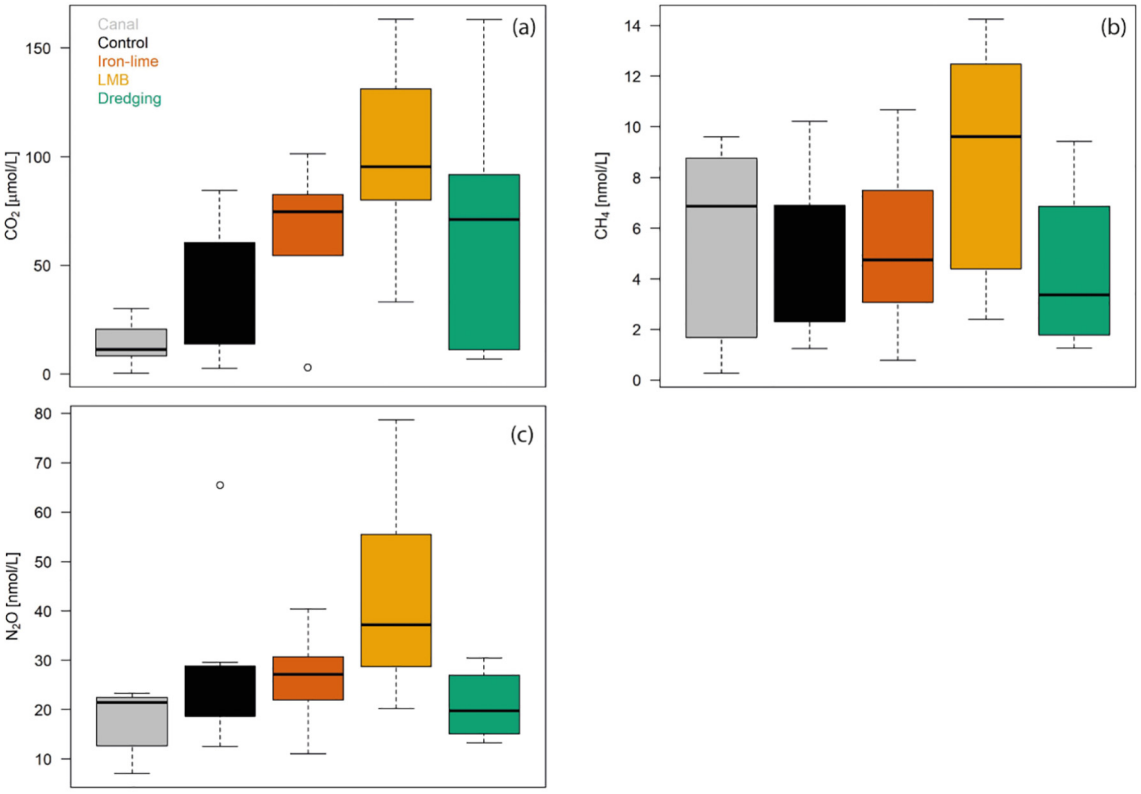

Fig. 6. Box plot (10%, 25%, 75% and 90% percentiles) of the concentrations of dissolved methane (a – CO_2), carbon dioxide (b – CH_4), and nitrous oxide (c – N_2O) at the end of the experiment (19-09-2019).

environmental complexity are few and far between. Here, we also evaluated how the efficacy of these interventions is impacted by exposure to an extreme heatwave in the middle of the experiment. This addressed the knowledge gap we currently face regarding the usefulness of commonly applied restoration measures under future climate scenarios. At the end of this discussion section, we will propose a conceptual model on potential routes through which measures to mitigate water quality deterioration might be affected by heatwaves. To our knowledge, such a comprehensive conceptual model is still lacking in literature and can provide a starting point for future validation.

The study site was a hypertrophic shallow water system according to the Carlson trophic state index (TSI; Carlson, 1977). The experiment focussed on the reduction of the internal loading as a means to mitigate water quality deterioration, with most of the external loading effectively blocked in our type of mesocosm. The experiment started at the end of June with rather high phytoplankton biomasses (initial total chlorophyll-a = 57.7 ± 1.3 μg/L) and depleted SRP concentrations (< 0.6 μg P/L), presumably due to high nutrient uptake by phytoplankton. Overall, the dissolved oxygen concentrations in the mesocosms decreased over the lifetime of the experiment, indicating that the systems were shifting from a primary production-dominant to a decomposition-dominant system.

4.1. Comparison of intervention measures

Among the tested four restoration treatments, the dredging treatments exhibited the greatest efficacy with respect to reduction of total phytoplankton biomass (evidenced by total chlorophyll-a), cyanobacteria biomass (evidenced by cyanobacteria chlorophyll-a), and improvement on water transparency (evidenced by Secchi depth). The dredging treatments aimed at removing the top nutrient-rich sediments, resulting in newly exposed sediments with lower nutrient release (estimate of the P loading = 0.2–0.7 P/m^2/day; Van Herpen, 2019). While the other three restoration measures only targeted immobilization of inorganic P, dredging of top 30-cm sediments will also result in a reduction of nitrogen (Fig. S1) and assimilable carbon in the organic matter that may facilitate microbial growth leading to oxygen depletion and release of redox-sensitive P (Yin et al., 2021). Moreover, there is increasing evidence that phytoplankton can also uptake organic nutrients for their growth (Bentzen et al., 1992; Boyer et al., 2006; Znachor and Nedoma, 2010). The anticipated decline in organic matter content in the newly exposed sediments may lead to decreased oxygen consumption, supported by the temporally increased DO and pH during the heatwave phase (Fig. 3). Such an increase of DO concentrations in the dredging treatments disappeared after the heatwave phase, which can be caused by the sedimentation of phytoplankton charging the newly exposed sediments with organic nutrients (Lürling and Faassen, 2012).

The lanthanum modified bentonite (LMB) treatments exhibited comparative efficacy compared with the dredging treatments, confirming the first hypothesis. We expected that the LMB treatments would immobilize SRP from the water columns into the sediments, which was not supported by the observations of SRP concentrations in the water column showing no distinct deviations from the control treatments. A rough estimate of P fluxes using the water column SRP data from July 12th and July 24th resulted in as high as 16 mg P/m^2/d in LMB treatments and 12 mg P/m^2/d in controls, and these estimates were even with uptake by phytoplankton. This level of P loading is much higher than the critical value for this system shifting from a clear state to a turbid state (estimate = 2.2 mg P/m^2/day; Van Herpen, 2019). The high P-fluxes in LMB treatments are probably due to ebullition of gas transporting sediment nutrients into water, evidenced by the relatively high CO_2 and CH_4 gas concentrations in LMB treatments (Fig. 6). Previous studies indicated that the ebullition of gases from sediments can be an important mechanism for nutrient transport from the sediment into overlying water in eutrophic lakes (Varjo et al., 2003). This result contrasts other studies that have shown a strong SRP reduction capacity of LMB, also under anoxia (e.g. Funes et al., 2021; Li et al., 2019), but finds support in another mesocosm study that observed hampered SRP binding by LMB (Lürling and Faassen, 2012). There may be several factors responsible for those deviating performances. The high pH at the start of the experiment (pH 9.7) implied strong competition between phosphate and hydroxyl ions for binding sites; the binding capacity of LMB at pH 9.5 is about one-third of the binding capacity at pH 7 (Li et al., 2019). Filterable La in the water column over the course of the experiment did not bind with SRP (Fig. 4d), which may be attributed to the presence of high DOC prevailing in eutrophic water bodies (background concentration in the canal = 6.37 ± 1.74 mg/L, unpublished data Water Authority Brabantse Delta), preventing phosphate precipitation by La-clay chelation (Lürling et al., 2014). Field observations from multiple lakes suggest that DOC concentrations negatively influence the efficacy of LMB (Spears et al., 2016) and such negative impacts by DOC will not disappear after 1 year (Dithmer et al., 2016). Note that although we observed overall higher La concentrations in the overlying water of the LMB treatments, they are far below the Dutch standard for surface water (10.1 μg La/L; Sneller et al., 2000) during most of the time except for one mesocosm which temporally exceeded the standard reaching 21 μg La/L on 12th of July, but dropped down to 2 μg La/L immediately at the next sampling. Our LMB results were in line with Li et al. (2019) demonstrating that the presence of phytoplankton can act as a P sink and thus hampering P adsorption by LMB. They found that an intensified dosage of LMB can mitigate such inference from phytoplankton. Moreover, Lürling and Faassen (2012) demonstrated that combined sediment dredging and LMB addition is a more promising measure than their treatments alone.

The iron-lime sludge exhibited a moderate efficacy, with a performance better than aeration but worse than dredging and LMB treatments, confirming our second hypothesis that the application of iron-lime sludge on the sediment is less effective in reducing phytoplankton biomass. Fe measurements of the water column as well as pore water (Fig. S2) showed iron-lime sludge did increase the Fe pool. The sediment P-fractionation results (Fig. S3a) showed that organic P is the second common P fraction after the redox-sensitive P accounting for approximately 35% of the mobile P. Mineralization of organic matter would exhaust the oxygen pool. Thus, the sediments were highly likely to be reducing (also reflected by the decreased DO concentrations in the iron-lime sludge treatments, Fig. 3a and Fig. S3b), leading to an increasing fraction of Fe^{2+} reducing P retention capacity of the sediment (Gächter and Müller, 2003). The optimum pH values for FeP binding is 4–5.5 (Kraal et al., 2015), while the CaP bond can dissolve under acidic conditions (Gon Kim et al., 2002; Ippolito et al., 2003). We observed no distinct difference in the calcium concentrations in the water column between the iron-lime sludge treatments and other treatments (Fig. S2), suggesting no CaP dissolution. Huang et al. (2005) demonstrated that P release in response to pH variations in lake sediments is dependent on a ratio of Fe-P content to Ca-P content, with high Fe-P/Ca-P ratio releasing P under alkaline conditions and low Fe-P/Ca-P ratio releasing more P under acidic conditions. In our Iron-lime sludge, Ca accounted for a larger proportion than Fe (Table S1), thus, being acidity-sensitive. However, the pH in the water columns remained high in our systems (pH > 8.8, Fig. 3c) presumably owing to the presence of a high phytoplankton biomass consuming inorganic carbon. Thus, in this system the efficacy of Iron-lime sludge is more likely to be redox-related than pH-related.

In agreement with our third hypothesis, the aeration treatments were unable to stimulate the iron trap of sediment phosphorus and hinder the growth of phytoplankton, with an end concentration comparable to the control mesocosms (Fig. 5). Previous studies demonstrated that any form of mixing of water columns in shallow water bodies (< 15 m) can lead to a negative effect on the water quality (Visser et al., 2016). This is because in such shallow water bodies (<2 m), oxygenation by air pumping will inevitably enhance sediment resuspension. The direct consequence of sediment resuspension is decrease in water clarity as reflected by the decreased Secchi depth in comparison to the control mesocosms (see Fig. 3b). Another unfavourable consequence of enhanced sediment resuspension may likely be sediment nutrients release, which will fuel the phytoplankton growth in the surface water. The favourable effect of aeration we expected was increased DO in the water columns and in the sediments, preventing release of redox-

sensitive P (Cavalcante et al., 2018). Based on the water column DO measurements (Fig. 3a, DO concentrations and Fig. S3b for DO saturation) as well as the pore water nutrient concentrations (Fig. 4b for SRP and Fig. S1 for NH_4-N and NO_2-N), we have to reject this hypothesis as we observed no distinct difference between the aeration treatment and the other treatments. This might be related to the large pool of organic matters in the sediments (Remke et al., 2018) and the observation that decomposition of resuspended sediment organic matters can lead to high DO consumption. Gächter and Wehrli (1998) demonstrated that oxygenation was unable to increase the P retention capacity of the sediment in presence of excessive organic matter. In conclusion, aeration is not a suitable measure in eutrophication control in shallow water system.

In addition to these four measures, the mesocosm treatment itself showed significant effects on water quality (grey area in Fig. 2). The direct consequences of mesocosm treatments are isolation from the surrounding canal water, which occasionally receives an inlet discharge of 0.06 m^3/s when the inlet was fully operated (Van Herpen, 2019). This resulted in a dramatic reduction of external nutrient loading (estimate = 2.77 mg P/m^2/day; Van Herpen, 2019), absence of fish (estimate = 772.8 kg/ha; Van Herpen, 2019), and shelter from wind resulting in decreased mixing of water and sediment resuspension (indicated by the increased Secchi depth in mesocosms, Fig. 3b). Absence of fish will lead to decreased grazing pressure on zooplankton (Jeppesen et al., 1997) and reduced bioturbation of sediments (Adámek and Maršálek, 2013). In a mesocosm experiment by Lürling et al. (2017) increased Rotifer and Cladocera abundances were observed, supporting this hypothesis. This could partly explain the lower phytoplankton abundance in the mesocosms owing to increased grazing pressure from zooplankton. The higher P loading in canals, however, did not translate to a relatively higher concentration of SRP relative to the mesocosm water. This is likely to be a result of the higher phytoplankton biomass in the canal resulting in larger amounts of P-uptake (Riegman, 1985).

4.2. Heatwave impacts on the internal P cycling

During the heatwave phase, we observed in all mesocosm treatments an increase of SRP concentrations in the water column by on average 270.3%, with a mean concentration of 30.1 μg P/L at the end of the experiment. Previous modelling studies (Janse, 2005) demonstrated that a SRP concentration of 50 μg P/L can result in an ecosystem shift from the clear state to the turbid state. This shows that the temperature effect detected in our data (a rise of the SRP concentration of 10 μg P/L/°C) is highly relevant. The increases in SRP concentrations coincided with increased phytoplankton biomass in the last month (Fig. 5) and decreased water transparency (Fig. 3b). However, the increases in phytoplankton biomass showed a lagged response to the increases in nutrient concentrations. This mismatch could be due to the previous depletion of environmental SRP concentrations resulting in a low internal nutrient content ('cell quota') in the phytoplankton cells (Droop, 1974). It likely took some time for the organisms to rebalance their cell quota resulting in a delayed response in their biomass. This phenomenon is modelled by the well-known Droop equation in ecological models (e.g. PCLake; Janse, 2005). A potential explanation for our observations is thus that sediment SRP release was taken up quickly once phytoplankton attained sufficient biomasses, resulting in a depleted SRP concentration in the water column until the end of the experiment. Evaluating this hypothesis on the nutrient uptake by phytoplankton is difficult in such in-situ mesocosm experimental set-up, where there is unlikely to be a control treatment for primary productivity. Our fourth hypothesis that the efficacy of iron-lime sludge will be hampered by increased water temperature was not rejected as was our fifth hypothesis that heatwave exposure resulted in P-release from lanthanum modified bentonite treated sediments. The heatwave-induced P-release was not re-immobilized despite the presence of available La (Fig. 4d), at least at a time scale of months. Similar results were observed in a previous laboratory study (Zhan et al., 2021), which supported our conclusion that the heatwave-induced P-release is long-lasting and will not disappear immediately post to heatwave. Additional experiments are needed to investigate the changes of LaP binding capacity upon heatwave exposure. Our sixth hypothesis that there is no heatwave effect on the efficacy of dredging is rejected as the dredging was shown to be unable to mitigate the heatwave-induced increases in P-releases. In summary, the efficacy of all the tested measures was reduced during the heatwave phase.

Greenhouse gas (GHG) emission of water bodies is substantial (Li et al., 2021; Rosentreter et al., 2021) and is promoted by eutrophication (Beaulieu et al., 2019; Davidson et al., 2015). Climate change might reduce the efficacy of interventions (Rolighed et al., 2016; Zhan et al., 2021), as indicated by this study as well. If interventions become less effective, water quality deteriorates even further, resulting in more GHG emissions (Li et al., 2021). These extra contributions to climate change pose a negative feedback to the efficacy of interventions. Thus, insight into the impact of interventions on GHG emissions is needed to reduce the reinforcing effect that eutrophication has on GHG emissions (Moss et al., 2011) and at the same time to provide an instrument for water managers to incorporate GHG emissions when selecting a treatment. Our dissolved GHG measurements indicated that LMB may not be a promising restoration measure in terms of mitigation of GHG emissions, given its overall higher GHG concentrations than other treatments (Fig. 6). It was unexpected that the LMB treatments showed higher GHG values than the control treatments given that LMB applications should not target organic carbon. A potential cause for this may be that the newly formed LMB layer on the top of sediments hampers oxygen penetration creating a favourable anoxic environment for microbial gas production. Surprisingly, the dredged mesocosms did not show a significant reduction in GHG concentrations with treatments other than LMB. We speculate that the dredging exposed sediments did not differ substantially in organic C content relative to the non-dredged sediments. This research gives an indication of GHG emissions caused by promising interventions (Fig. 6), though GHG flux of ebullition needs to be incorporated to provide an accurate estimation of the GHG emissions from sediments.

We propose a graphical model illustrating the underlying mechanisms for heatwave impacts on the efficacy of intervention measures (Fig. 7). In general, the P cycle can be divided into two compartments, one representing a biological P loop that involves P fluxes between organic P and labile P via biological processes (i.e. decomposition and primary production), another representing a chemical P loop that involves P fluxes between chemical bound P (including Lanthanum bound P; redox-sensitive P: Fe/Mn-P; and pH-sensitive P: Al/Fe-P) and labile P via chemical sorption and desorption processes. Our results indicated that heatwave exposure increased the phosphorus pools stored in the biological loop, whereas the phosphorus pools in the chemical loop decreased.

The heatwave effect can play a role in phosphorus cycling through several mechanisms. Firstly, increasing temperature enhances decomposition of organic matter and release of detrital nutrients (Gudasz et al., 2010). Furthermore, the decreased oxygen concentrations as a result of enhanced mineralization and respiration could lead to anoxic conditions at the sediment resulting in release of redox-sensitive phosphorus (Fe- and Mn-bound P; Cavalcante et al., 2018).

In addition, increasing DOC levels resulting from decomposition of organic matter has been found to interfere with the precipitations of LaP (Lürling et al., 2014; Spears et al., 2016) and CaP (Cao et al., 2007; Sindelar et al., 2015), thus, decreasing phosphorus immobilization via these pathways. Lei et al. (2018) suggests that high pH can overcome the negative DOC effects on CaP. The pH level is elevated owing to increased primary production and enhanced uptake of inorganic carbon. High pH would facilitate desorption of pH-sensitive P (Fe-/Al-P). Some laboratory experiments demonstrated negative impacts of high pH on the P removal efficacy of LMB (Kang et al., 2021), and attributed it to competition with hydroxyl ions for binding sites. However, the pH

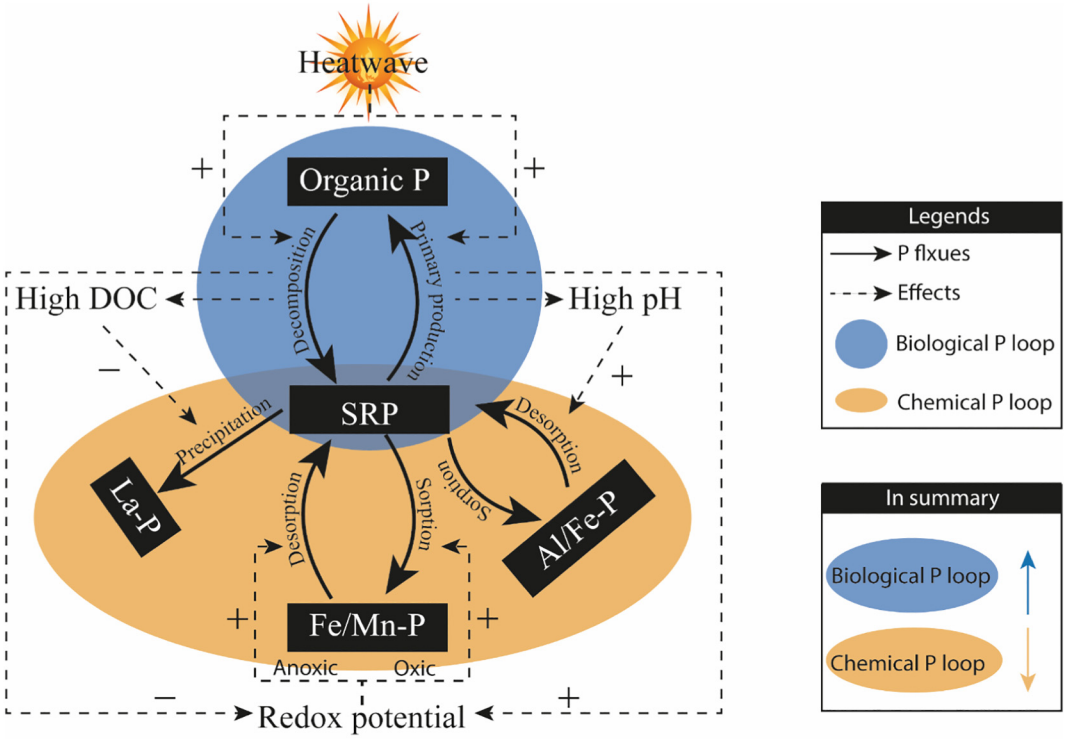

Fig. 7. Conceptual model illustrating the interaction between environmental conditions and internal phosphorus cycling. The solid lines represent the P fluxes between different P forms. The dashed lines with the "+" and "-" are the positive or negative effects on P fluxes during a heatwave event.

effects on Ca-/La- P precipitation are either established in short laboratory experiments or far from reaching a consensus. Thus, we decided not to include the pH effects on Ca-/La- P precipitation in our model.

With phosphorus pools locked in the biological loop, the chemical immobilization of labile P was inhibited. This maybe especially true for summer conditions, when temperatures are high and primary production is intensive, a high amount of P is stored in organisms, hampering the P-adsorption efficacy of chemical adsorbents, which underpins the importance of planning restoration activities during periods when most P is not already stored in biota. It is anticipated that inland waters may have prolonged growing seasons with a higher risk of long-lasting algal blooms under the effects of global warming, which is currently, however, rarely taken into consideration by lake managers when applying restoration measures (Jeppesen et al., 2007). In addition, warm lakes tend to be more productive than similar cold lakes, with everything else equal (Jeppesen et al., 2020). Our results on this temperate shallow urban water system could provide implications for eutrophication management of tropical lakes when selecting treatments, in which the restoration efforts are much limited compared to the lakes in the temperate zone (Thornton, 1987). Our results suggest that the intervention measures that only target SRP might take longer in inhibiting phytoplankton biomass in temperate systems when applied during warm periods with high rates of biological processes, whereas they might not be promising in tropical systems with no period where there is low organismal biomass (i.e. perannual growth).

Knowledge about the influence of temperature on chemical P binding capacity is lacking. Although it is hypothesized that warmer water can facilitate interactions between chemical compounds through increased kinetic energy, such positive temperature effects on P binding capacity are not conclusive for LMB and aluminium salts (Kang et al., 2021). We hypothesize that in highly productive systems temperature effects on biological processes are more important to nutrient cycling when compared with the direct temperature effects on the chemical nutrient de−/sorption, as most of the nutrients exist in organic forms. For these reasons, the temperature effects on chemical reactions are not included in our conceptual model.

5. Conclusions, caveats and recommendations

Using a replicated near-real world mesocosm study, we tested the efficacy of four restoration measures to control internal P-loading in a hypertrophic shallow urban system impacted by an extreme summer heatwave. Our sampling time interval was rather large for an event analysis, with high frequency measurements likely providing a more detailed insight on the water quality dynamics of the restored water.

Notwithstanding the limitations of our sampling regime, we were able to derive a conceptual model that explains the underlying pathways that determine the cycling of phosphorus between different forms, which can improve our understanding and prediction of the efficacy of restoration measures under future climate scenarios. Measurements of more variables such as dissolved organic carbon and the sediment redox potential are needed for validating the proposed conceptual model.

The take home messages of our study:

1. Dredging and Lanthanum modified bentonite are more effective than iron-lime sludge in decreasing phytoplankton biomass and improving water clarity.
2. Near-sediment aeration was not able to stimulate the iron trap in the sediment in shallow water systems.
3. The efficacy of the tested measures was hampered by a heatwave. We speculate that the heatwave, through its accelerating impacts on biogeochemical processes, locked P pools in the biological loop, i.e. the exchange between labile P and organic P. As a consequence, the efficacy of P adsorbents is hampered due to reduced P pools in the chemical loop.
4. As intervention measures that only target SRP may likely take longer in inhibiting phytoplankton biomass during warmer periods, we recommend an application strategy before the growing season (autumn or early spring in temperate systems) when the biological P loop is less prominent relative to the chemical P loop.

In conclusion, our results suggest that our current efforts on eutrophication control are very likely to be compromised under global warming, and

more research on how to adapt our restoration measures to a warming world is needed.

CRediT authorship contribution statement

Qing Zhan: Conceptualization, Methodology, Software, Formal analysis, Writing – original draft, Visualization. **Sven Teurlincx:** Methodology, Formal analysis, Investigation, Resources, Data curation, Writing – review & editing, Project administration. **Frank van Herpen:** Resources, Writing – review & editing. **Nandini Vasantha Raman:** Investigation. **Miquel Lürling:** Validation, Writing – review & editing. **Guido Waajen:** Validation, Resources, Writing – review & editing. **Lisette N. de Senerpont Domis:** Conceptualization, Methodology, Validation, Writing – original draft, Supervision, Project administration.

Declaration of competing interest

The authors declare that they have no known competing financial interests or personal relationships that could have appeared to influence the work reported in this paper.

Acknowledgements

We want to thank Machiel van Halsteren, Erik Reichman, Dennis Waasdorp and Nico Helmsing for assistance in the field campaign and sample analyses. This research was designed and carried out in collaboration with independent consultancy Royal HaskoningDHV (https://global.royalhaskoningdhv.com/), and in particular with Boris Smulders and Niels Schoffelen. This research was commissioned and funded by Waterboard Brabantse Delta, in collaboration with the municipality of Geertruidenberg. Specifically, we are grateful for Henk Kools of the municipality of Geertruidenberg, and Simon Hofstra, Henk van Laarhoven en Louis Vriens of the Waterboard Brabantse Delta for the co-design of the study. Q. Zhan was funded by the European Union's Horizon 2020 Research and Innovation Programme under the Marie Skłodowska-Curie grant agreement no. 722518 (MANTEL ITN) and the Royal Netherlands Academy of Arts and Sciences (KNAW).

Appendix A. Supplementary data

Supplementary data to this article can be found online at https://doi.org/10.1016/j.scitotenv.2022.154421.

References

Adámek, Z., Maršálek, B., 2013. Bioturbation of sediments by benthic macroinvertebrates and fish and its implication for pond ecosystems: a review. Aquac. Int. 21, 1–17.

Babin, J., Prepas, E.E., Murphy, T.P., Serediak, M., Curtis, P.J., Zhang, Y., Chambers, P.A., 1994. Impact of lime on sediment phosphorus release in hard water lakes: the case of hypereutrophic Halfmoon Lake, Alberta. LakeReserv.Manag. 8, 131–142. https://doi.org/10.1080/07438149409354465.

Beaulieu, J.J., Del Sontro, T., Downing, J.A., 2019. Eutrophication will increase methane emissions from lakes and impoundments during the 21st century. Nat. Commun. 10, 1375. https://doi.org/10.1038/s41467-019-09100-5.

Bentzen, E., Taylor, W.D., Millard, E.S., 1992. The importance of dissolved organic phosphorus to phosphorus uptake by limnetic plankton. Limnol. Oceanogr. 37, 217–231.

Biggs, J., von Fumetti, S., Kelly-Quinn, M., 2017. The importance of small waterbodies for biodiversity and ecosystem services: implications for policy makers. Hydrobiologia 793, 3–39. https://doi.org/10.1007/s10750-016-3007-0.

Bolund, P., Hunhammar, S., 1999. Ecosystem services in urban areas. Ecol. Econ. 29, 293–301.

Boström, B., 1984. Potential mobility of phosphorus in different types of lake sediment. Int. Rev.Ges.Hydrobiol.Hydrogr. 69, 457–474. https://doi.org/10.1002/iroh.19840690402.

Boyer, J.N., Dailey, S.K., Gibson, P.J., Rogers, M.T., Mir-Gonzalez, D., 2006. The role of dissolved organic matter bioavailability in promoting phytoplankton blooms in Florida Bay. Hydrobiologia 569, 71–85. https://doi.org/10.1007/s10750-006-0123-2.

Cabrerizo, M.J., Álvarez-Manzaneda, M.I., León-Palmero, E., Guerrero-Jiménez, G., de Senerpont Domis, L.N., Teurlincx, S., González-Olalla, J.M., 2020. Warming and CO2 effects under oligotrophication on temperate phytoplankton communities. Water Res. 173, 115579. https://doi.org/10.1016/j.watres.2020.115579.

Cao, X., Harris, W.G., Josan, M.S., Nair, V.D., 2007. Inhibition of calcium phosphate precipitation under environmentally-relevant conditions. Sci. Total Environ. 383, 205–215.

Carlson, R.E., 1977. A trophic state index for lakes 1. Limnol. Oceanogr. 22, 361–369.

Carpenter, S.R., 2008. Phosphorus control is critical to mitigating eutrophication. Proc. Natl. Acad. Sci. 105, 11039–11040.

Carpenter, S.R., Ludwig, D., Brock, W.A., 1999. Management of eutrophication for lakes subject to potentially irreversible change. Ecol. Appl. 9, 751–771. https://doi.org/10.1890/1051-0761(1999)009[0751:MOEFLS]2.0.CO;2.

Cavalcante, H., Araújo, F., Noyma, N.P., Becker, V., 2018. Phosphorus fractionation in sediments of tropical semiarid reservoirs. Sci. Total Environ. 619–620, 1022–1029. https://doi.org/10.1016/j.scitotenv.2017.11.204.

Chorus, I., Falconer, I.R., Salas, H.J., Bartram, J., 2000. Health risks caused by freshwater cyanobacteria in recreational waters. J.Toxicol.Environ.HealthBCrit.Rev. 3, 323–347.

Team, R.C., 2019. R: A Language And Environment for Statistical Computing.

Copetti, D., Finsterle, K., Marziali, L., Stefani, F., Tartari, G., Douglas, G., Reitzel, K., Spears, B.M., Winfield, I.J., Crosa, G., 2016. Eutrophication management in surface waters using lanthanum modified bentonite: a review. Water Res. 97, 162–174.

Cowell, B.C., Dawes, C.J., Gardiner, W.E., Scheda, S.M., 1987. The influence of whole lake aeration on the limnology of a hypereutrophic lake in central Florida. Hydrobiologia 148, 3–24.

Davidson, T.A., Audet, J., Svenning, J.-C., Lauridsen, T.L., Søndergaard, M., Landkildehus, F., Larsen, S.E., Jeppesen, E., 2015. Eutrophication effects on greenhouse gas fluxes from shallow-lake mesocosms override those of climate warming. Glob. Chang. Biol. 21, 4449–4463. https://doi.org/10.1111/gcb.13062.

Dithmer, L., Nielsen, U.G., Lundberg, D., Reitzel, K., 2016. Influence of dissolved organic carbon on the efficiency of P sequestration by a lanthanum modified clay. Water Res. 97, 39–46.

Droop, M.R., 1974. The nutrient status of algal cells in continuous culture. J. Mar. Biol. Assoc. U. K. 54, 825–855. https://doi.org/10.1017/S002531540005760X.

Funes, A., Álvarez-Manzaneda, I., Arco, A.D., de Vicente, J., de Vicente, I., 2021. Evaluating the effect of CFH-12® and Phoslock® on phosphorus dynamics during anoxia and resuspension in shallow eutrophic lakes. Environ. Pollut. 269. https://doi.org/10.1016/j.envpol.2020.116093.

Gächter, R., Müller, B., 2003. Why the phosphorus retention of lakes does not necessarily depend on the oxygen supply to their sediment surface. Limnol. Oceanogr. 48, 929–933. https://doi.org/10.4319/lo.2003.48.2.0929.

Gächter, R., Wehrli, B., 1998. Ten years of artificial mixing and oxygenation: no effect on the internal phosphorus loading of two eutrophic lakes. Environ. Sci. Technol. 32, 3659–3665. https://doi.org/10.1021/es980418l.

Geurts, J.J.M., Smolders, A.J.P., Banach, A.M., van de Graaf, J.P.M., Roelofs, J.G.M., Lamers, L.P.M., 2010. The interaction between decomposition, net N and P mineralization and their mobilization to the surface water in fens. Water Res. 44, 3487–3495. https://doi.org/10.1016/j.watres.2010.03.030.

Ghasemi, A., Zahediasl, S., 2012. Normality tests for statistical analysis: a guide for non-statisticians. Int.J.Endocrinol.Metab. 10, 486.

Golterman, H.L., 1997. The distribution of phosphate over iron-bound and calcium-bound phosphate in stratified sediments. Hydrobiologia 364, 75–81. https://doi.org/10.1023/A:1003159924052.

Gon Kim, J., Hyun Kim, J., Moon, H.-S., Chon, C.-M., Sung Ahn, J., 2002. Removal capacity of water plant alum sludge for phosphorus in aqueous solutions. Chem.Speciat.Bioavailab. 14, 67–73.

Grolemond, G., Wickman, H., 2011. Dates and times made easy with lubridate. J. Stat. Softw. 40, 1–25.

Gudasz, C., Bastviken, D., Steger, K., Premke, K., Sobek, S., Tranvik, L.J., 2010. Temperature-controlled organic carbon mineralization in lake sediments. Nature 466, 478–481. https://doi.org/10.1038/nature09186.

Halbedel, S., 2015. Protocol for CO2 sampling in waters by the use of the headspace equilibration technique, based on the simple gas equation; second update. https://doi.org/10.1038/protex.2015.085.

Holtan, H., Kamp-Nielsen, L., Stuanes, A.O., 1988. Phosphorus in soil, water and sediment: an overview. Phosphorus in Freshwater Ecosystems, pp. 19–34.

Huang, Q., Wang, Z., Wang, C., Wang, S., Jin, X., 2005. Phosphorus release in response to pH variation in the lake sedimentswith different ratios of iron-bound P to calcium-bound P. Chem.Speciat.Bioavailab. 17, 55–61. https://doi.org/10.3184/095422905782774937.

Hupfer, M., Zak, D., Roβberg, R., Herzog, C., Pöthig, R., 2009. Evaluation of a well-established sequential phosphorus fractionation technique for use in calcite-rich lake sediments: identification and prevention of artifacts due to apatite formation. Limnol. Oceanogr. Methods 7, 399–410. https://doi.org/10.4319/lom.2009.7.399.

Ippolito, J.A., Barbarick, K.A., Heil, D.M., Chandler, J.P., Redente, E.F., 2003. Phosphorus retention mechanisms of a water treatment residual. J. Environ. Qual. 32, 1857–1864.

Jankowski, T., Livingstone, D.M., Bührer, H., Forster, R., Niederhauser, P., 2006. Consequences of the 2003 European heat wave for lake temperature profiles, thermal stability, and hypolimnetic oxygen depletion: implications for a warmer world. Limnol. Oceanogr. 51, 815–819. https://doi.org/10.4319/lo.2006.51.2.0815.

Janse, J.H., 2005. Model Studies on the Eutrophication of Shallow Lakes And Ditches [publisher not identified], Wageningen.

Jeppesen, E., Lauridsen, T., Mitchell, S.F., Burns, C.W., 1997. Do planktivorous fish structure the zooplankton communities in New Zealand lakes? N. Z. J. Mar. Freshw. Res. 31, 163–173.

Jeppesen, E., Søndergaard, M., Meerhoff, M., Lauridsen, T.L., Jensen, J.P., 2007. Shallow lake restoration by nutrient loading reduction—some recent findings and challenges ahead. Shallow Lakes in a Changing World. Springer, pp. 239–252.

Jeppesen, E., Canfield, D.E., Bachmann, R.W., Søndergaard, M., Havens, K.E., Johansson, L.S., Lauridsen, T.L., Sh, T., Rutter, R.P., Warren, G., Ji, G., Hoyer, M.V., 2020. Toward predicting climate change effects on lakes: a comparison of 1656 shallow lakes from

Florida and Denmark reveals substantial differences in nutrient dynamics, metabolism, trophic structure, and top-down control. Inland Waters 10, 197–211. https://doi.org/10.1080/20442041.2020.1711681.

Jeppesen, E., Audet, J., Davidson, T.A., Neif, É.M., Cao, Y., Filiz, N., Lauridsen, T.L., Larsen, S.E., Beklioğlu, M., Sh, T., Søndergaard, M., 2021. Nutrient loading, temperature and heat wave effects on nutrients, oxygen and metabolism in shallow lake mesocosms pre-adapted for 11 years. Water 13, 127. https://doi.org/10.3390/w13020127.

Kang, L., Mucci, M., Lürling, M., 2021. Influence of temperature and pH on phosphate removal efficiency of different sorbents used in lake restoration. Sci. Total Environ. 151489. https://doi.org/10.1016/j.scitotenv.2021.151489.

Kraal, P., Burton, E.D., Rose, A.L., Kocar, B.D., Lockhart, R.S., Grice, K., Bush, R.T., Tan, E., Webb, S.M., 2015. Sedimentary iron–phosphorus cycling under contrasting redox conditions in a eutrophic estuary. Chem. Geol. 392, 19–31. https://doi.org/10.1016/j.chemgeo.2014.11.006.

Lei, Y., Song, B., Saakes, M., Van Der Weijden, R.D., Buisman, C.J., 2018. Interaction of calcium, phosphorus and natural organic matter in electrochemical recovery of phosphate. Water Res. 142, 10–17.

Li, X., Zhang, Z., Xie, Q., Yang, R., Guan, T., Wu, D., 2019. Immobilization and release behavior of phosphorus on phoslock-inactivated sediment under conditions simulating the photic zone in eutrophic shallow lakes. Environ. Sci. Technol. 53, 12449–12457. https://doi.org/10.1021/acs.est.9b04093.

Li, Y., Shang, J., Zhang, C., Zhang, W., Niu, L., Wang, L., Zhang, H., 2021. The role of freshwater eutrophication in greenhouse gas emissions: a review. Sci. Total Environ. 768, 144582. https://doi.org/10.1016/j.scitotenv.2020.144582.

Lin, J., Qiu, P., Yan, X., Xiong, X., Jing, L., Wu, C., 2015. Effectiveness and mode of action of calcium nitrate and Phoslock® in phosphorus control in contaminated sediment, a microcosm study. Water Air Soil Pollut. 226, 330. https://doi.org/10.1007/s11270-015-2590-4.

Lindstrom, M.J., Bates, D.M., 1988. Newton—Raphson and EM algorithms for linear mixed-effects models for repeated-measures data. 83, pp. 1014–1022. https://doi.org/10.1080/01621459.1988.10478693 null.

Lürling, M., Faassen, E.J., 2012. Controlling toxic cyanobacteria: Effects of dredging and phosphorus-binding clay on cyanobacteria and microcystins. Water Res. 46, 1447–1459. https://doi.org/10.1016/j.watres.2011.11.008 Cyanobacteria: Impacts of climate change on occurrence, toxicity and water quality management.

Lürling, M., Mucci, M., 2020. Mitigating eutrophication nuisance: in-lake measures are becoming inevitable in eutrophic waters in the Netherlands. Hydrobiologia https://doi.org/10.1007/s10750-020-04297-9.

Lürling, M., Waajen, G., van Oosterhout, F., 2014. Humic substances interfere with phosphate removal by lanthanum modified clay in controlling eutrophication. Water Res. 54, 78–88.

Lürling, M., Waajen, G., Engels, B., van Oosterhout, F., 2017. Effects of dredging and lanthanum-modified clay on water quality variables in an enclosure study in a hypertrophic pond. Water (Switzerland) 9, 380. https://doi.org/10.3390/w9060380.

Lürling, M., Mello, M.M.e, van Oosterhout, F., de Senerpont Domis, L., Marinho, M.M., 2018. Response of natural cyanobacteria and algae assemblages to a nutrient pulse and elevated temperature. Front. Microbiol. 9, 1851. https://doi.org/10.3389/fmicb.2018.01851.

Magen, C., Lapham, L.L., Pohlman, J.W., Marshall, K., Bosman, S., Casso, M., Chanton, J.P., 2014. A simple headspace equilibration method for measuring dissolved methane. Limnol. Oceanogr. Methods 12, 637–650. https://doi.org/10.4319/lom.2014.12.637.

Mooij, W.M., De Senerpont Domis, L.N., Hülsmann, S., 2008. The impact of climate warming on water temperature, timing of hatching and young-of-the-year growth of fish in shallow lakes in the Netherlands. J. Sea Res. 60, 32–43. https://doi.org/10.1016/j.seares.2008.03.002 Dynamics of Fish and Fishers.

Moss, B., Kosten, S., Meerhoff, M., Battarbee, R.W., Jeppesen, E., Mazzeo, N., Havens, K., Lacerot, G., Liu, Z., De Meester, L., 2011. Allied attack: climate change and eutrophication. Inland Waters 1, 101–105.

Mucci, M., Maliaka, V., Noyma, N.P., Marinho, M.M., Lürling, M., 2018. Assessment of possible solid-phase phosphate sorbents to mitigate eutrophication: influence of pH and anoxia. Sci. Total Environ. 619, 1431–1440.

Noble, A., Hassall, C., 2015. Poor ecological quality of urban ponds in northern England: causes and consequences. Urban Ecosyst. 18, 649–662.

Oksanen, J., Blanchet, F.G., Friendly, M., Kindt, R., Legen, P., McGlinn, D., R. Minchin, P., Hara, R.B.O., Simpson, G.L., Solymos, P., Stevens, M.H.H., Szoecs, E., Wagner, H., 2019. vegan: Community Ecology Package.

Paerl, H.W., Huisman, J., 2008. Blooms like it hot. Science 320, 57–58.

Pinheiro, J., Bates, D., DebRoy, S., Sarkar, D., Team, R.C., 2019. nlme: Linear And Nonlinear Mixed Effects Models.

Psenner, R., Pucsko, R., Sage, M., 1984. Fractionation of organic and inorganic phosphorus compounds in lake sediments, an attempt to characterize ecologically important fractions (Die Fraktionierung Organischer und Anorganischer Phosphorverbindungen von Sedimenten, Versuch einer Definition Okologisch Wichtiger Fraktionen). Arch. Hydrobiol. 1.

Remke, E., Lucassen, E., Smolders, F., 2018. Effectiveness of iron lime sludge - column experiment (No. RP-18.018.18.79).

Riegman, R., 1985. Phosphate-phytoplankton Interactions. Universiteit van Amsterdam (PhD Thesis).

Rolighed, J., Jeppesen, E., Søndergaard, M., Bjerring, R., Janse, J.H., Mooij, W.M., Trolle, D., 2016. Climate change will make recovery from eutrophication more difficult in shallow Danish Lake Søbygaard. Water 8, 459. https://doi.org/10.3390/w8100459.

Rosentreter, J.A., Borges, A.V., Deemer, B.R., Holgerson, M.A., Liu, S., Song, C., Melack, J., Raymond, P.A., Duarte, C.M., Allen, G.H., Olefeldt, D., Poulter, B., Battin, T.I., Eyre, B.D., 2021. Half of global methane emissions come from highly variable aquatic ecosystem sources. Nat. Geosci. 14, 225–230. https://doi.org/10.1038/s41561-021-00715-2.

Schindler, D.W., Hecky, R.E., Findlay, D.L., Stainton, M.P., Parker, B.R., Paterson, M.J., Beaty, K.G., Lyng, M., Kasian, S.E.M., 2008. Eutrophication of lakes cannot be controlled by reducing nitrogen input: results of a 37-year whole-ecosystem experiment. Proc. Natl. Acad. Sci. 105, 11254–11258.

Shatwell, T., Thiery, W., Kirillin, G., 2019. Future projections of temperature and mixing regime of European temperate lakes. Hydrol. Earth Syst. Sci. 23, 1533–1551. https://doi.org/10.5194/hess-23-1533-2019.

Sindelar, H.R., Brown, M.T., Boyer, T.H., 2015. Effects of natural organic matter on calcium and phosphorus co-precipitation. Chemosphere 138, 218–224.

Smith, V.H., Schindler, D.W., 2009. Eutrophication science: where do we go from here? Trends Ecol. Evol. 24, 201–207.

Smolders, A.J., Lucassen, E.C., Van Der Aalst, M., Lamers, L.P., Roelofs, J.G., 2008. Decreasing the abundance of Juncus effusus on former agricultural lands with noncalcareous sandy soils: possible effects of liming and soil removal. Restor. Ecol. 16, 240–248.

Sneller, F.E.C., Kalf, D.F., Weltje, L., Van Wezel, A.P., 2000. Maximum permissible concentrations and negligible concentrations for rare earth elements (REEs).

Søndergaard, M., Bjerring, R., Jeppesen, E., 2013. Persistent internal phosphorus loading during summer in shallow eutrophic lakes. Hydrobiologia 710, 95–107.

Spears, B.M., Mackay, E.B., Yasseri, S., Gunn, L.D.M., Waters, K.E., Andrews, C., Cole, S., De Ville, M., Kelly, A., Meis, S., Moore, A.L., Nurnberg, G.K., van Oosterhout, F., Pitt, J.A., Madgwick, G., Woods, H.J., Lurling, M., 2016. A meta-analysis of water quality and aquatic macrophyte responses in 18 lakes treated with lanthanum modified bentonite (Phoslock (R)). Water Res. 97, 111–121. https://doi.org/10.1016/j.watres.2015.08.020.

Stockwell, J.D., Doubek, J.P., Adrian, R., Anneville, O., Carey, C.C., Carvalho, L., De Senerpont Domis, L.N., Dur, G., Frassl, M.A., Grossart, H.-P., 2020. Storm impacts on phytoplankton community dynamics in lakes. Glob. Chang. Biol. 26, 2756–2784.

Teurlincx, S., Kuiper, J.J., Hoevenaar, E.C.M., Lurling, M., Brederveld, R.J., Veraart, A.J., Janssen, A.B.G., Mooij, W.M., Domis, L.N.D., 2019. Towards restoring urban waters: understanding the main pressures. Curr. Opin. Environ. Sustain. 36, 49–58. https://doi.org/10.1016/j.cosust.2018.10.011.

Thornton, J.A., 1987. Aspects of eutrophication management in tropical/sub-tropical regions. J.Limnol.Soc.South.Afr. 13, 25–43. https://doi.org/10.1080/03779688.1987.9634541.

Tukey, J.W., 1949. Comparing individual means in the analysis of variance. Biometrics 99–114.

Van den Brink, P.J., Braak, C.J.T., 1999. Principal response curves: analysis of time-dependent multivariate responses of biological community to stress. Environ.Toxicol.Chem. 18, 138–148.

Van Herpen, F., 2019. Blue-green Algae in De Veste (No. BF5862-101–100). Royal Haskoning DHV.

Varjo, E., Liikanen, A., Salonen, V.-P., Martikainen, P.J., 2003. A new gypsum-based technique to reduce methane and phophorus release from sediments of eutrophied lakes: (Gypsum treatment to reduce internal loading). Water Res. 37, 1–10. https://doi.org/10.1016/S0043-1354(02)00264-6.

Verpoorter, C., Kutser, T., Seekell, D.A., Tranvik, L.J., 2014. A global inventory of lakes based on high-resolution satellite imagery. Geophys. Res. Lett. 41, 6396–6402. https://doi.org/10.1002/2014GL060641.

Visser, P.M., Ibelings, B.W., Bormans, M., Huisman, J., 2016. Artificial mixing to control cyanobacterial blooms: a review. Aquat. Ecol. 50, 423–441. https://doi.org/10.1007/s10452-015-9537-0.

Waajen, G.W.A.M., 2017. Eco-engineering for Clarity: Clearing Blue-green Ponds And Lakes in an Urbanized Area. University https://doi.org/10.18174/406887.

Waajen, G.W.A.M., Faassen, E.J., Lürling, M., 2014. Eutrophic urban ponds suffer from cyanobacterial blooms: Dutch examples. Environ. Sci. Pollut. Res. 21, 9983–9994. https://doi.org/10.1007/s11356-014-2948-y.

Waajen, M.L.G., Engels, B., Oosterhout, F.V., 2017. Effects of dredging and lanthanum-modified clay on water quality variables in an enclosure study in a hypertrophic pond. Water 9, 380.

Waldman, D.M., 1983. A note on algebraic equivalence of White's test and a variation of the Godfrey/Breusch-Pagan test for heteroscedasticity. Econ. Lett. 13, 197–200.

Wickham, H., François, R., Henry, L., Müller, K., 2019. dplyr: A Grammar of Data Manipulation. R Package Version 0.8. 0.1 Retrieved January 13, 2020.

Wong, B., 2011. Points of view: color blindness. Nat. Methods 8. https://doi.org/10.1038/nmeth.1618 441-441.

Woolway, R.I., Kraemer, B.M., Lenters, J.D., Merchant, C.J., O'Reilly, C.M., Sharma, S., 2020. Global lake responses to climate change. Nat.Rev.Earth Environ. 1–16.

Woolway, R.I., Jennings, E., Shatwell, T., Golub, M., Pierson, D.C., Maberly, S.C., 2021. Lake heatwaves under climate change. Nature 589, 402–407. https://doi.org/10.1038/s41586-020-03119-1.

Yin, H., Yang, C., Yang, P., Kaksonen, A.H., Douglas, G.B., 2021. Contrasting effects and mode of dredging and in situ adsorbent amendment for the control of sediment internal phosphorus loading in eutrophic lakes. Water Res. 189, 116644. https://doi.org/10.1016/j.watres.2020.116644.

Yuan, H., Tai, Z., Li, Q., Liu, E., 2020. In-situ, high-resolution evidence from water-sediment interface for significant role of iron bound phosphorus in eutrophic lake. Sci. Total Environ. 706, 136040. https://doi.org/10.1016/j.scitotenv.2019.136040.

Zhan, Q., Stratmann, C.N., van der Geest, H.G., Veraart, A.J., Brenzinger, K., Lürling, M., de Senerpont Domis, L.N., 2021. Effectiveness of phosphorus control under extreme heatwaves: implications for sediment nutrient releases and greenhouse gas emissions. Biogeochemistry https://doi.org/10.1007/s10533-021-00854-z.

Znachor, P., Nedoma, J., 2010. Importance of dissolved organic carbon for phytoplankton nutrition in a eutrophic reservoir. J. Plankton Res. 32, 367–376. https://doi.org/10.1093/plankt/fbp129.